ISSN 1024-8560, Atmospheric and Oceanic Optics, 2023, Vol. 36, No. 4, pp. 329–336. © Pleiades Publishing, Ltd., 2023.
Russian Text © The Author(s), 2023, published in Optika Atmosfery i Okeana.

REMOTE SENSING OF ATMOSPHERE, HYDROSPHERE, AND UNDERLYING SURFACE

Variability of Parameters of Single-Layer Cloud Fields over Western Siberia in Summer for the Period from 2001 to 2019 According to MODIS Data

V. G. Astafurov[a], *, A. V. Skorokhodov[a], **, and K. V. Kuryanovich[a], ***

[a] *V.E. Zuev Institute of Atmospheric Optics, Siberian Branch, Russian Academy of Sciences, Tomsk, 634055 Russia*

**e-mail: astafurov@iao.ru*

***e-mail: vazime@yandex.ru*

****e-mail: ksuyain@mail.ru*

Received July 27, 2022; revised December 30, 2022; accepted January 25, 2023

Abstract—Long-term variability of the parameters of single-layer cloud fields over Western Siberia in summer from 2001 to 2019 is estimated based on MODIS data. The seasonal mean cloud cover and cloud parameters (optical thickness, effective radius of particles, waterpath, and top height) are estimated for different single-layer cloud types by the results of cloud classification from summer (June–August) daily satellite images of the target region. Parameters of single-layer clouds are analyzed for three latitudinal zones of Western Siberia: southern (<60° N), transitional (60°–65° N), and northern (>65° N). The linear trends in the cloud cover and in cloud parameters are found for different single-layer cloud types from the long-term data series. Convective and low-level clouds in the northern and transition zone of the region under study are characterized by maximal variability of the above parameters. The effect of anomalous blocking anticyclones on some cloud parameters is shown for different cloud types in the considered latitudinal zones of Western Siberia.

Keywords: Western Siberia, single-layer clouds, physical parameters, long-term trend, satellite data, blocking anticyclone

DOI: 10.1134/S1024856023040048

INTRODUCTION

Clouds cover 60–70% of the Earth's surface every day [1, 2]. They directly participate in different processes in the "atmosphere–ocean–land" system, including hydrological cycle, radiative transfer, aerosol transport, etc. Therefore, cloudiness is one of the main objects of research in climatology and meteorology. Cloud fields are heterogeneous; they can attain several thousand kilometers in length. According to the modern meteorological standard, there are 27 cloud forms, including 10 main types, their subtypes, and certain combinations [3]. This classification of clouds is based on the morphological description of their types when observing from the ground, which is described in the Cloud Atlas [4]. However, the occurrence of each cloud type is due to specific causes, which include internal waves, convection, convergence, and general atmospheric circulation processes (for example, jet streams, fronts, and cyclones) [5]. Therefore, information about the high frequency of certain cloud types over a region within a long time period can indicate the predominance of certain atmospheric processes there. A variation in the cloudiness regime over a region can be considered a marker of the current climate changes.

There are more than 10 databases containing information on the variability of the parameters of mainly total and low-level cloudiness both over individual regions and over the Earth [1, 2, 6–8]. It seems appropriate to mention the works by Komarov [9–11] in relation to the territory of Western Siberia as an example of the detailed analysis of the frequency of low-level clouds. The current results of studying individual cloud types and their parameters over the territory of the Russian Federation were derived on the basis of ground-based and aircraft observations and are limited to the early 1990s. [5]. The acquisition of more recent data on the long-term variability of the parameters of specific cloud types is difficult because of the reduction in the number of meteorological stations and the occasional character of aircraft measurements [12]. An obvious solution to this problem is to use the data of Earth's remote sounding from space. But different characteristics of instruments used and algorithms for thematic data processing make it difficult to study the long-term variability of cloud field parameters. However, there are unique series of homogeneous satellite data

Table 1. Cloud classification

No.	Name	Designation
	Convective clouds	
1	Cumulus humilis	*Cu hum*
2	Cumulus medium and congestus	*Cu med/cong*
3	Cumulonimbus calvus	*Cb calv*
4	Cumulonimbus capillatus	*Cb cap*
	Low-level clouds	
5	Stratocumulus cumuliformes	*Sc cuf*
6	Stratocumulus undulates	*Sc und*
7	Stratus	*St*
8	Nimbostratus	*Ns*
	Mid-level clouds	
9	Altostratus	*As*
10	Altocumulus cumuliformes	*Ac cuf*
11	Altocumulus undulates	*Ac und*
	High-level clouds	
12	Cirrus fibratus	*Ci fib*
13	Cirrus spissatus	*Cisp*
14	Cirrostratus	*Cs*
15	Cirrocumulus	*Cc*

received with the same instruments, e.g., MODIS, during several decades, which allow reliable estimation of variations in cloud parameters from a climatological point of view.

Western Siberia is one of the key regions—indicators of the global climate change. Satellite and ground-based measurements and reanalysis data show a significant increase in the number of temperature anomalies here over the past decades [13]. The regional topography favors this process. The West Siberian Plain is a low-lying heavily swampy and forested territory. It is bounded by the Ural Mountains in the west, the Central Siberian Plateau in the east, the Arctic Ocean in the north, Kazakh Upland in the south, and foothills of Altai and the Western Sayan Mountains in the southeast [14]. This special geographical position creates conditions for the development of a pronounced meridional transport, which intensifies under conditions of extensive blocking anticyclones over the European Russia or the Asian (Siberian) anticyclone in winter [15, 16]. Therefore, Western Siberia is characterized by significant temperature fluctuations throughout the year and long periods of the abnormally hot or cold weather. The increase in the number of temperature anomalies in this region is accompanied by a simultaneous reduction in the area of old sea ice in the Russian Arctic and swamping of the forest tundra and tundra [17, 18]. One can assume a change in the cloudiness regime in Western Siberia over the past decades due to the strengthening/weakening of the processes occurring in the “atmosphere–ocean–land” system. These changes should have affected both total cloudiness in general and multi- and single-layer clouds in particular.

The aim of this work is to analyze the long-term variability of the parameters of single-layer cloud fields over Western Siberia in summer based on satellite data from 2001 to 2019.

SOURCE DATA

For the comprehensive analysis of the long-term variability of the parameters of single-layer cloudiness fields, we consider the following latitudinal zones of Western Siberia: southern (<60° N), transitional (60°–65° N), and northern (>65° N). The MODIS data obtained in June–August 2001–2019 were used as the main source of information on cloud parameters over the region under study. The *Terra* and *Aqua* satellites, where the MODIS spectroradiometer is mounted, cross the equator at 03:30 and 06:30 UTC in the considered time zone. This makes it possible to cover almost the entire region with one or two successive daily images at an off-nadir angles of no more than 40°, which excludes from consideration distortions at the edges of images due to the survey geometry [19].

Table 1 shows the combined summer cloud classification used in this work. We suggested this classification in [20] taking into account the meteorological standard and MODIS spectroradiometer parameters, in particular, its spatial resolution. Though the number of cloud types have been decreased from 27 to 15 in this classification, it allows identifying almost all processes in the "atmosphere–ocean–land" system, where clouds are generated. Thus, stratocumulus (*Sc cuf* and *Sc und*) and altocumulus (*Ac cuf* and *Ac und*) subtypes belong to the same types (*Sc* and *Ac*, respectively), but they are resulted from different processes. Cumuliform clouds (*Sc cuf* and *Ac cuf*) are formed due to convection, while undulated clouds (*Sc und* and *Ac und*), due to generation and propagation of Kelvin–Helmholtz waves [4]. Thus, the cloud classification presented makes it possible to identify the predominance of both mesoscale (for example, internal waves and convection) and more global processes (for example, atmospheric fronts and cyclones) over a regions of the planet.

We use daytime MODIS images with a spatial resolution of 250 m (0.62–0.67 μm); MOD06_L2 and MYD06_L2 thematic products with a spatial resolution of 1000 m, which contain cloud parameters; and MOD03 and MYD03 georeference files. The following cloud parameters are considered: optical thickness (τ), effective radius of particles (r_{eff}), waterpath (P), and top height (h_{ct}). In addition, the seasonal mean cloud cover n_S(type) was determined for different single-layer cloud types for the latitudinal zones of Western Siberia from 2001 to 2019. The decision on the simultaneous presence of clouds at one or several layers is made based on the value of the corresponding flag in MOD06_L2 and MYD06_L2 data products. For the consistency of the results of retrieval of the cloud parameters between *Terra* and *Aqua*, we used data sets compiled from data of the 2.2- and 11-μm bands [21]. The value of the solar zenith angle can be neglected in each individual case, since the construction of long-term trends in the cloud parameters under study implies the coverage of a large amount of information [22].

ANALYSIS TECHNIQUE

The technique for analyzing the long-term variability of the parameters of single-layer cloud fields over the latitudinal zones of Western Siberia is based on the results of recognition of 15 cloud types from Table 1 in daily MODIS images. Clouds are classified using the probabilistic neural network described in [20], which allows cloud type recognition with a probability of 0.85 in daytime satellite images made in the absence of snow cover. This probability value is among the highest for this region [23]. The recognition result is a pseudocolor MODIS image, where each color corresponds to a certain cloud type.

The boundaries of the latitudinal zones of Western Siberia considered in the work are superimposed on a satellite image obtained after the cloud classification procedure. After processing all the data for each target region, the seasonal mean cloud cover for different single-layer clouds from Table 1 is estimated as

$$n_{\text{S}}(\text{type}) = \frac{\sum_{i=1}^{M} \frac{s_{\text{type},i}}{s_i}}{M},$$

where "type" is the cloud type identifier from Table 1; M is the number of images processed for three summer months of each year; $s_{\text{type},\,i}$ is the number of pixels in the zone belonging to this cloud type in the ith day; s_i is the size of the zone in pixels. The seasonal mean fraction of single-layer cloudiness is calculated as

$$\nu_{\text{S}} = \frac{\sum_{i=1}^{M} \frac{\sum_{\text{type}} s_{\text{type},i}}{s_i}}{M}.$$

Similarly, based on the data of MOD06_L2 and MYD06_L2 data products, annual seasonal estimates of the means of the parameters $\langle\tau\rangle_{\text{S}}$, $\langle r_{\text{eff}}\rangle_{\text{S}}$, $\langle P\rangle_{\text{S}}$ and $\langle h_{\text{ct}}\rangle_{\text{S}}$ are calculated for different cloud types for each latitudinal zone of Western Siberia. During the final stage, the long-term trends in the above cloud parameter are found.

RESULTS AND DISCUSSION

According to the MODIS data processing results, the long-term seasonal mean cloud cover by single-layer clouds $\nu_{\text{S}} = 40\%$ for the northern zone of Western Siberia, 41% for the transitional zone, and 38% for the southern zone. Figure 1 shows long-term series of n_{S}(type) values for some cloud types from different layers according to Table 1. The analysis of the results allows us to drawn several conclusions. The contrast in the values of the seasonal mean cloud coverage is higher between the northern and transitional zones than between the transitional and southern zones for such cloud types as *Cu hum* (Fig. 1a), *Sc und* (Fig. 1b), *Cu med/cong*, *Cb cap*, *St*, *Ns*, *Ci fib*, and *Cc*. For most of them, $h_{\text{ct}} = 2.5$ km; therefore, we can assume that these zonal differences in n_{S}(type) are due to changes in the temperature regime of the underlying surface. Most of Western Siberia is covered by *Cu hum*, *Sc cuf*, *Sc und*, *Ns*, and *Ac cuf* clouds in summer. Moreover, in the northern zone, n_{S}(type) is higher for clouds generated by internal waves (*Sc und* and *Ac und*), and in the south, for clouds generated under the effect of convection (*Cu hum* and *Sc cuf*). For high-level clouds, the contrast of the seasonal mean cloud cover between the latitudinal zones under study is less pronounced. Note that the estimates of n_{S}(type) do not contradict the information on the frequency of individual cloud types before the early 1990s, derived from regular ground-

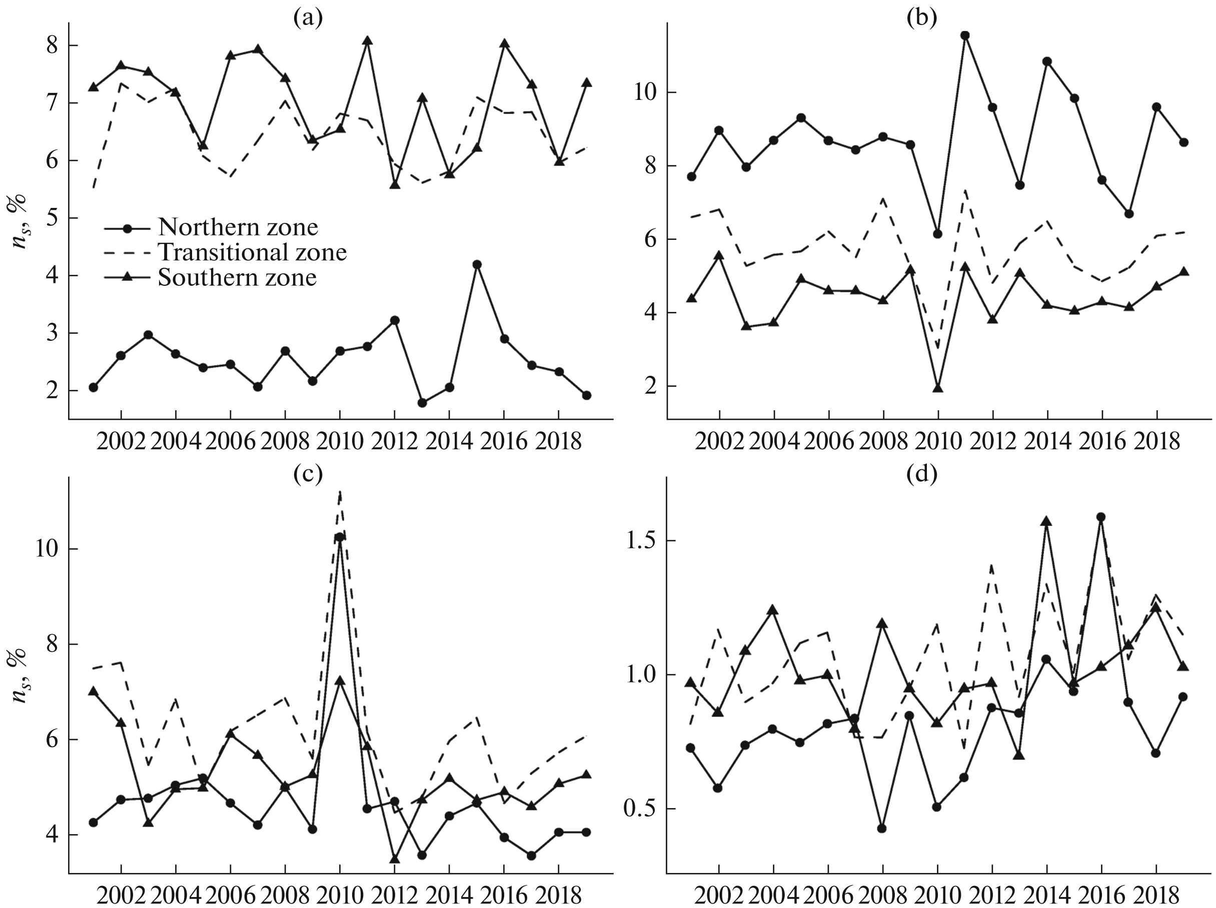

Fig. 1. Seasonal mean cloud cover for (a) *Cu hum*, (b) *Sc cuf*, (c) *Ac cuf*, and (d) *Cs* of the latitudinal zones of Western Siberia under study in summer.

based and aircraft observations [5], and complement the observations.

In addition, Fig. 1 shows abnormal n_S values in 2010 for some cloud types (*Sc und* and *Ac cuf*) in all latitudinal zones of the region under study. Similar outbursts have been recorded for *Cb calv* and *Ac und*. That time, an anticyclone was observed over the European Russia for 55 days [24, 25]. Matching these events, we can put forward a hypothesis that an increase in meridional transport against the background of blocking the western transport leads to a change in the horizontal dimensions of mesoscale processes, namely, internal waves and convection. Thus, the seasonal mean cloud cover for *Sc und* clouds generated by Kelvin–Helmholtz waves decreased by 2% on the average throughout Western Siberia (Fig. 1b), and for *Ac cuf* clouds, which are originated due to convection, on the contrary, increased by approximately 4% in each latitudinal zone. It is noteworthy that the seasonal mean cloud cover of the territory of Western Siberia by deep convection *Cb calv* and *Cb cap* clouds was the lowest in 2010 throughout the period under study. Anomalies in the generation of convective cloudiness during periods of atmospheric blocking were also noted in [26, 27].

Table 2 includes estimates of the characteristics of the linear trend in the relative cloud cover of underlying surface by single-layer clouds of different types

$$\Delta_n(\text{type}) = \frac{a_n \Delta t}{\langle n_S(\text{type}) \rangle},$$

where a_n are the slopes of the trend line found by the least-squares method from n_S(type) values from 2001 to 2019; $\langle n_S(\text{type}) \rangle$ is the long-term mean. For the convenience of practical use of the results, it is accepted that $\Delta t = 10$. Cloud subtypes with low n_S values or a neutral trend in all zones were not included in Table 2.

A pronounced decrease in the cloud cover of the region under study by low-level and mid-level single-layer clouds in summer, especially by stratus forms, is seen from Table 2. A decrease in the amount of low-level clouds in summer throughout Western Siberia was also found in [11] based on data from ground-based weather stations. The amount of convective and cirrus clouds barely changes mainly in the northern

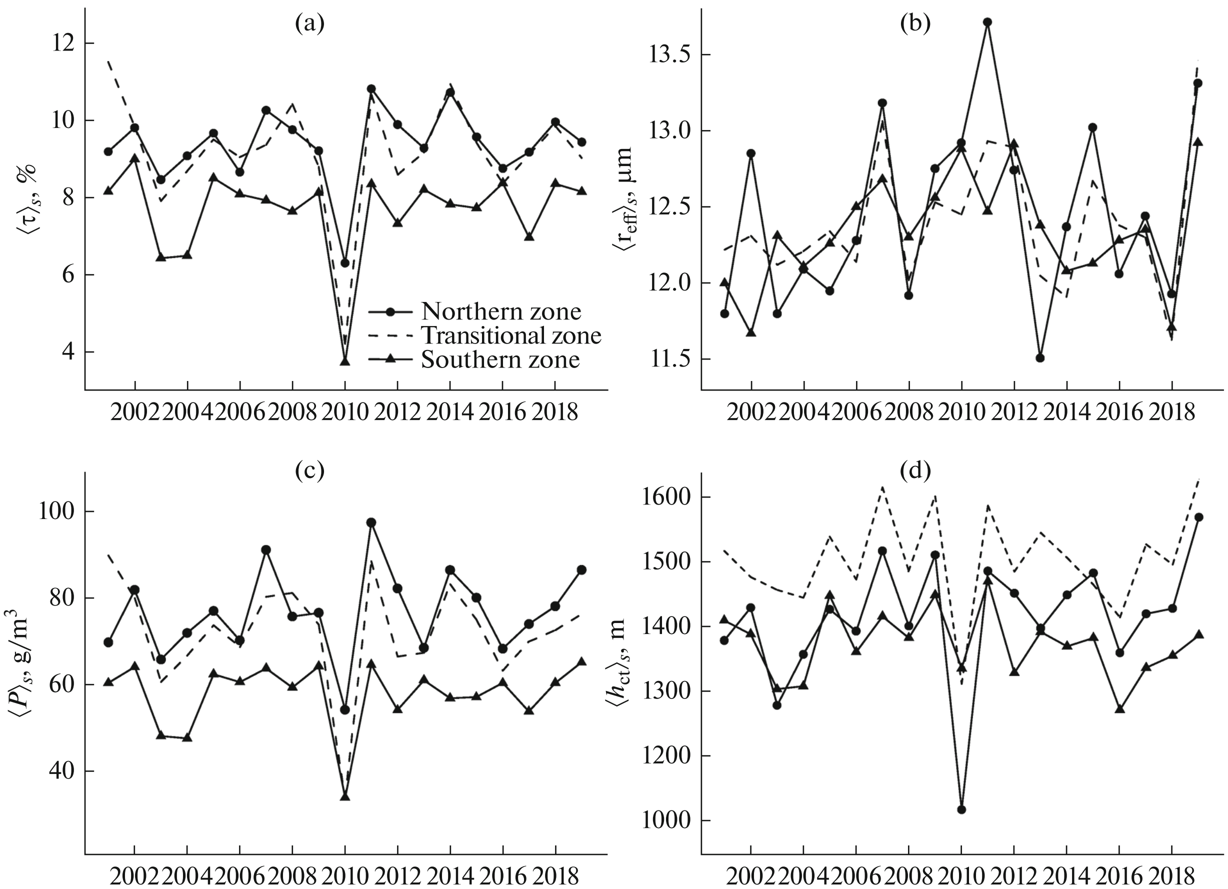

Fig. 2. Long-term variability of the (a) optical thickness, (b) effective radius of cloud particles, (c) waterpath, and d) cloud top height for *Sc und* over different latitudinal zones of Western Siberia in summer (from 2001 to 2019).

and transitional zones. Analyzing Table 2, we can conclude that single-layer cloudiness regime was the most stable over the period under study in the southern zone of Western Siberia.

Figure 2 shows long-term variability of $\langle\tau\rangle_S$, $\langle r_{eff}\rangle_S$, $\langle P\rangle_S$, and $\langle h_{ct}\rangle_S$ for *Sc und* clouds. These dependences are in good agreement with the changes in n_S(*Sc und*), except for the effective radius of cloud particles (see Fig. 1b). However, the differences in the above cloud parameters between the latitudinal zones under study is less pronounced than in n_S(type). Note that the $\langle\tau\rangle_S$, $\langle r_{eff}\rangle_S$, $\langle P\rangle_S$, and $\langle h_{ct}\rangle_S$ values for *Sc und* do not go beyond the allowable ranges given in the well-known reference literature on clouds [4, 5, 28]. In addition,

Table 2. Estimates of the characteristics of the linear trend in n_S(type) for different cloud types and long-term mean $\langle n_S(\text{type})\rangle_{\Delta t}$

Cloud type	$\Delta_n/\langle n_S\rangle$, %		
	Northern zone	Transitional zone	Southern zone
Cu hum	N	N	−0.06/7.0
Sc cuf	−0.05/4.6	−0.15/6.1	−0.07/6
Sc und	0.02/8.7	−0.05/5.7	N
Ns	−0.10/6.7	N	N
Ac cuf	−0.11/4.7	−0.13/6.2	−0.11/5.3
Ac und	−0.17/3.4	−0.14/3.0	−0.04/2.6
Cc	–	N	0.03/2.9

"–" corresponds to $\langle n_S\rangle < 2\%$; "N" means the neutral trend in the cloud cover at $|\Delta_n| < 0.02$.

Table 3. Estimates of the characteristics of a linear trend in $\langle\tau\rangle_S$ and $\langle P\rangle_S$ for different cloud types and long-term mean $\langle\langle\tau\rangle_S\rangle$ and $\langle\langle P\rangle_S\rangle$

Cloud type	Northern zone	Transitional zone	Southern zone
	$\Delta_\tau/\langle\langle\tau\rangle_S\rangle$		
Cu hum	0.03/10	−0.02/9.7	−0.02/8.9
Cb calv	0.03/30	N	N
Cb cap	N	−0.03/52	−0.03/50
Sc cuf	0.03/9.1	N	H
Sc und	0.02/9.4	−0.02/9.2	N
St	−0.03/12	0.09/11	N
Ns	0.02/20	N	N
As	N	0.03/17	−0.03/21
Ac und	N	N	0.04/7.2
Ci fib	0.04/2.8	0.03/2.8	0.04/2.7
Cs	0.08/2.4	0.04/2.2	0.08/2.2
Cc	0.03/3.8	0.03/3.9	0.05/3.9
	$\Delta_P/\langle\langle P\rangle_S\rangle$, g/m^2		
Cu hum	N	−0.05/88	−0.02/76
Cu med/cong	−0.04/780	−0.03/560	−0.02/460
Cb calv	N	N	−0.03/588
Cb cap	−0.03/1490	−0.06/1430	−0.03/1280
Sc cuf	0.03/78	−0.03/67	N
Sc und	0.04/77	−0.03/72	0.02/58
St	−0.03/117	−0.07/83	N
Ns	0.05/185	−0.03/208	−0.03/188
As	0.03/300	−0.03/337	−0.03/355
Ac cuf	N	−0.03/199	N
Ac und	N	N	0.04/62
Cisp	N	−0.02/486	N
Cs	0.02/57	0.04/55	0.06/50
Cc	N	N	0.02/57

"N" means the neutral trend in $\langle\tau\rangle_S$ or $\langle P\rangle_S$ at $|\Delta_\tau| < 0.02$ or $|\Delta_P| < 0.02$, respectively.

Fig. 2 shows responses of the parameters of *Sc und* clouds and n_S(*Sc und*) to atmospheric blocking events in 2010, except for the effective radius of particles. Moreover, the seasonal mean $\langle\tau\rangle_S$, $\langle P\rangle_S$, and $\langle h_{ct}\rangle_S$ decrease in response to atmospheric blocking over the European Russia presumably due to a decrease in the height of the temperature inversion layers, over which *Sc und* clouds are generated, with an increase in the pressure. Abnormal values of the cloud parameters (mainly optical thickness and waterpath) were observed in different latitude zones not only in 2010, but also in 2012 (for example, for *Cu hum*), under the conditions of long-lived anticyclone over the territory of Western Siberia.

Let us estimate the accuracy of the results of retrieval of the seasonal mean cloud cover of the region under study by different cloud types and cloud parameters. As a measure of error, we consider the relative mean-square error δ. Thus, $\delta(n_S) = 3\%$; $\delta(\langle\tau\rangle_S) = 5\%$; $\delta(\langle r_{eff}\rangle_S) = 3\%$, $\delta(\langle P\rangle_S) = 6\%$; and $\delta(\langle h_{ct}\rangle_S) = 6\%$ for *Sc und* in 2019 in the transition zone. For other cloud types, estimates of δ have close values.

Table 3 shows estimates of the relative long-term variability of $\langle\tau\rangle_S$ and $\langle P\rangle_S$ for different cloud types over the latitudinal zones of Western Siberia under study. The $\Delta\tau$ and ΔP values are calculated similarly to Δn. Here, $\langle\langle\cdot\rangle_S\rangle$ means successive averaging over the season and over long-term series of observations. Table 3 shows a general increase in the optical thickness of low-level and high-level clouds throughout Western Siberia. Values of $\langle\tau\rangle_S$ of convective clouds increase in the northern zone and decrease in other zones, while the optical thickness of mid-level clouds has a neutral trend throughout Western Siberia. In the northern zone, the τ values decrease only in *St*. The analysis of Table 3 allows us to conclude that convective clouds are characterized by neutral and negative trends in waterpath in all latitudinal zones, while low-level and mid-level clouds, only in the transition zone. The waterpath decreases for all cloud types which make the main contribution to the total amount of precipitation in the season under study (*Cu*, *Cb*, and *Ns*).

The effective radius of cloud particles is characterized by weaker variability than the optical thickness and waterpath. A slight (2–5%) decrease in $\langle r_{\text{eff}} \rangle_{\text{S}}$ in *Cu med/cong*, *Cb calv*, and *As* and an increase in this parameter in *St* are observed in all the zones. The cloud top height increases for convective cloudiness and low-level clouds throughout Western Siberia. The growth of $\langle h_{\text{ct}} \rangle_{\text{S}}$ in July near deep convection clouds over the region under study is discussed in [29]. A predominantly negative trend in this parameter is characteristic of mid-level clouds in all zones. However, the variability of $\langle h_{\text{ct}} \rangle_{\text{S}}$ is the greatest in *Cu hum*, *St*, and *As* clouds.

The most significant changes in the parameters under study are observed for convective and low-level clouds in the northern and transition zones. This gives grounds to assume relationships between these phenomena and an increase in the number of temperature anomalies in these zones over the past two decades [13]. Confirmation of this hypothesis can be considered as a promising direction for further work.

CONCLUSIONS

The main result of the work is the assessment of the long-term variability of the parameters of different cloud types over certain latitudinal zones of Western Siberia. Some peculiarities of the change in the single-layer cloudiness regime over the region under study in 2001–2019 have been ascertained. A reduction in the cloud cover of Western Siberia has been revealed for low-level and mid-level clouds; other cloud types are characterized by neutral trends. The seasonal variability of the cloud parameters is maximal for convective and low-level clouds in the northern and transition zones. This fact might well be associated with an increase in the number of temperature anomalies in the region under study [13], since the temperature of the underlying surface is one of the key factors of origination of these cloud types. A reduction in the waterpath in clouds which produce the greatest amount of precipitation, i.e., *Cu*, *Cb*, and *Ns*, can be a marker of the climate change in Western Siberia. The optical depth of high-level clouds and their top height also increase in all latitudinal zones of Western Siberia. To estimate the absolute values of the above changes in the cloudiness regime, one can use the average values from Tables 2 and 3.

The study of the long-term variability of the parameters of single-layer cloud fields has shown the occurrence of abnormal values of n_{S}(type), $\langle \tau \rangle_{\text{S}}$, $\langle r_{\text{eff}} \rangle_{\text{S}}$, $\langle P \rangle_{\text{S}}$, and $\langle h_{\text{ct}} \rangle_{\text{S}}$ for some cloud types in one or simultaneously several latitudinal zones of Western Siberia in 2010 and 2012. Based on this, we assume an increase in the contribution of mesoscale processes to the formation of the cloudiness regime over the target region during periods of weakening/strengthening of the meridional transport against the background of blocking the western transport by long-lived anticyclones. Moreover, against the background of the events of 2010, the cloud cover of Western Siberia by undulating clouds decreased, and by clouds originated under the effect of convective processes, increased. A more detailed analysis of these phenomena is a promising direction for further work.

The results can be considered an actual source of information on single-layer cloudiness when solving climatological and meteorological problems for Western Siberia.

FUNDING

The work was supported by the Ministry of Science and Higher Education of the Russian Federation (V.E. Zuev Institute of Atmospheric Optics, Siberian Branch, Russian Academy of Sciences).

CONFLICT OF INTEREST

The authors declare that they have no conflicts of interest.

REFERENCES

1. C. J. Stubenrauch, W. B. Rossow, S. Kinne, S. Ackerman, G. Cesana, H. Chepfer, L. Di Girolamo, B. Getzewich, A. Guignard, A. Heidinger, B. C. Maddux, W. P. Menzel, P. Minnis, C. Pearl, S. Platnick, C. Poulsen, J. Riedi, S. Sun-Mack, A. Walther, D. Winker, S. Zeng, and G. Zhao, "Assessment of global cloud datasets from satellites: Project and database initiated by the GEWEX Radiation Panel," Bull. Am. Meteorol. Soc. **94** (7), 1031–1049 (2013).
2. A. V. Chernokul'skii and I. I. Mokhov, "Comparative analysis of the parameters of global and zonal clouds according to different satellite and ground-based observations," Issled. Zemli Kosmosa, No. **3**, 12–29 (2010).
3. *KN-01 SYNOP. Code for Prompt Transmission of Surface Meteorological Observation Data from the Roshydromet Station Network,* Ed. by N.P. Fakhrutdinov (Gidromettsentr Rossii, Moscow, 2013) [in Russian].
4. D. P. Bespalov, A. M. Devyatkin, Yu. A. Dovgalyuk, V. I. Kondratyuk, Yu. V. Kuleshov, T. P. Svetlova, S. S. Suvorov, and V. I. Timofeev, *Cloud Atlas* (D'ART, St. Petersburg, 2011) [in Russian].
5. *Clouds and Cloudy Atmosphere*. Handbook, Ed. by I.P. Mazin and A.Kh. Khrgian (Gidrometeoizdat, Leningrad, 1989) [in Russian].

6. R. A. Schiffer and W. B. Rossow, "The International Satellite Cloud Climatology Project (ISCCP): The first project of the world climate research programme," Bull. Am. Meteorol. Soc. **64** (7), 779–784 (1983).
7. C. Hahn, S. Warren, J. London, R. Jenne, and R. Chervin, Climatological Data for Clouds Over the Globe from Surface Observations (1988) (NDP-026) [Data set]. https://doi.org/10.3334/CDIAC/CLI.NDP026
8. M. D. King, S. Platnick, W. P. Menzel, S. A. Ackerman, and P. A. Hubanks, "Spatial and temporal distribution of clouds observed by MODIS Onboard the Terra and Aqua Satellites," IEEE Trans. Geosci. Remote Sens. **51**, 3826–3852 (2013).
9. V. S. Komarov, S. N. Il'in, A. V. Lavrinenko, N. Ya. Lomakina, E. V. Gorev, and D. P. Nakhtigalova, "Climate conditions of low clouds over the territory of Siberia and its modern change. Part 1. Features of low clouds conditions," Opt. Atmos. Okeana **26** (7), 579–583 (2013).
10. V. S. Komarov, D. P. Nakhtigalova, S. N. Il'in, A. V. Lavrinenko, and N. Ya. Lomakina, "Climatic zoning of the Siberia territory according to the total and lower cloudiness conditions as a basis for construction of local cloud atmosphere models. Part 1. Methodical bases," Opt. Atmos. Okeana **27** (10), 895–898 (2014).
11. V. S. Komarov, G. G. Matvienko, S. N. Il'in, and N. Ya. Lomakina, "Estimate of local features of long-term variations in cloud cover over the territory of Siberia using results of its climatic zoning according to total and low-level cloud regimes," Atmos. Ocean. Opt. **28** (3), 265–272 (2015).
12. A. S. Azarov, Yu. A. Borisov, B. G. Danelyan, V. V. Petrov, A. A. Sin'kevich, M. A. Strunin, B. A. Fomin, and V. Ch. Khattatov, "New opportunities in the study of atmospheric processes and environmental monitoring provided by the Yak-42D Roshydromet aircraft laboratory," in *Proc. of the All-Russian Open Conference on Cloud Physics and Active Effects on Hydrometeorological Processes* (Pechatnyi dvor, Nal'chik, 2015), pp. 48–58 [in Russian].
13. https://earthobservatory.nasa.gov/global-maps/MOD_LSTAD_M. Cited July 20, 2022.
14. E. V. Kharyutkina, S. V. Loginov, E. I. Usova, and Yu. V. Martynova, "Tendencies in changes of climate extremality in Western Siberia at the end of the XX century and the beginning of the XXI century," Fundam. Prikl. Klimatol., No. 2, 45–65 (2019).
15. A. V. Chernokulsky, I. I. Mokhov, and N. G. Nikitina, "Winter cloudiness variability over Northern Eurasia related to the Siberian High during 1966–2010," Environ. Res. Lett. **8** (4), 045012 (2013).
16. I. I. Mokhov, A. V. Chernokul'skii, and M. A. Osipov, "Atmospheric centers of action in the Northern and Southern Hemispheres: Features and variability," Russ. Meteorol. Hydrol. **45** (11), 749–761 (2020).
17. E. V. Shalina and L. P. Bobylev, "Sea ice transformations in the Arctic from satellite observations," Sovremennye Problemy Distantsionnogo Zondirovaniya Zemli Kosmosa **14** (6), 28–41 (2017).
18. T. B. Titkova and V. V. Vinogradova, "Climate changes in transitional natural areas of Russian northern regions and their display in landscape spectral characteristics," Sovremennye Problemy Distantsionnogo Zondirovaniya Zemli Kosmosa **16** (5), 310–323 (2019).
19. W. L. Barnes, T. S. Pagano, and V. V. Salomonson, "Prelaunch characteristics of the Moderate Resolution Imaging Spectroradiometer (MODIS) on EOS-AM1," IEEE Trans. Geosci. Remote Sens. **36** (20), 1088–1100.
20. A. V. Skorokhodov, V. G. Astafurov, and T. V. Evsyutkin, "Application of statistical models of the image textures and physical parameters of clouds for their classification on satellite imagery MODIS," Issled. Zemli Kosmosa, No. **4**, 43–58 (2018).
21. S. A. Ackerman, R. Frey, A. Heidinger, Y. Li, A. Walther, S. Platnick, K. G. Meyer, G. Wind, N. Amarasinghe, C. Wang, B. Marchant, R. Holz, S. Dutcher, and P. Hubanks, *EOS MODIS and SNPP VIIRS Cloud Properties: User Guide for the Climate Data Record Continuity Level-2 Cloud Top and Optical Properties Product (CLDPROP)* (NASA, Greenbelt, USA, 2019).
22. B. C. Maddux, S. A. Ackerman, and S. Platnick, "Viewing geometry dependencies in MODIS cloud products," J. Atmos. Ocean. Tech. **27**, 1519–1528.
23. R. Tapakis and A. G. Charalambides, "Equipment and methodologies for cloud detection and classification: A review," Solar Energy **95**, 392–430 (2013).
24. I. I. Mokhov, "Specific features of the 2010 summer heat formation in the European territory of Russia in the context of general climate changes and climate anomalies," Izv., Atmos. Ocean. Phys. **47** (6), 653–660 (2011).
25. N. P. Shakina and A. R. Ivanova, "The blocking anticyclones: The state of studies and forecasting," Russ. Meteorol. Hydrol. **35** (11), 721–730 (2010).
26. S. Mohr, J. Wandel, S. Lenggenhager, and O. Martius, "Relationship between atmospheric blocking and warm-season thunderstorms over Western and Central Europe," Q. J. R. Meteorol. Soc. **145** (724), 3040–3056 (2019).
27. A. Chernokulsky, A. Shikhov, A. Bykov, N. Kalinin, M. Kurgansky, B. Sherstyukov, and Y. Yarinich, "Diagnosis and modelling of two destructive derecho events in European Russia in the summer of 2010," Atmos. Res. **267**, 105928 (2019).
28. Yu. L. Matveev, L. T. Matveev, and S. A. Soldatenko, *Global Cloud Field* (Gidrometeoizdat, Leningrad, 1986) [in Russian].
29. A. V. Chernokulsky, A. V. Eliseev, F. A. Kozlov, N. N. Korshunova, M. V. Kurgansky, I. I. Mokhov, V. A. Semenov, N. V. Shvets', A. N. Shikhov, and Yu. I. Yarinich, "Atmospheric severe convective events in Russia: Changes observed from different data," Meteorol. Gidrol., No. 5, 27–41 (2022).